Identification of excited states and collectivity in ^{88}Se

I. N. Gratchev,[1,2] G. S. Simpson,[1] G. Thiamova,[1] M. Ramdhane,[1] K. Sieja,[3] A. Blanc,[2] M. Jentschel,[2] U. Köster,[2] P. Mutti,[2]
T. Soldner,[2] G. de France,[4] C. A. Ur,[5] and W. Urban[6]

[1]*LPSC, Université Grenoble Alpes, CNRS/IN2P3, Institut National Polytechnique de Grenoble, F-38026 Grenoble Cedex, France*
[2]*Institut Laue-Langevin, 71 avenue des Martyrs, 38042 Grenoble Cedex 9, France*
[3]*Université de Strasbourg, IPHC, 23 rue du Loess 67037 Strasbourg, CNRS, UMR7178, 67037 Strasbourg, France*
[4]*Grand Accélérateur National d'Ions Lourds, CEA/DRF–CNRS/IN2P3, Boulevard Henri Becquerel, F-14076 Caen, France*
[5]*INFN, via Marzolo 8, 35131 Padova, Italy*
[6]*Faculty of Physics University of Warsaw, ulica Pasteura 5, PL-02-093 Warsaw, Poland*

The γ decays of excited states in the very neutron-rich nucleus ^{88}Se have been observed following the neutron-induced fission of ^{235}U. The measurement was performed using the EXILL array of Ge detectors at the PF1B cold-neutron beam facility of the Institut Laue-Langevin, Grenoble. The level scheme of ^{88}Se was established using γ-γ-γ coincidences. A low (2_1^+) energy hints at the onset of quadrupole deformation, and the identification of possible members of a (2_2^+) band provide evidence for γ vibrations. Shell-model calculations using a ^{78}Ni core reproduce the decay scheme well. Equivalent deformation and $B(E2)$ values have previously been predicted for ^{88}Se using pseudo-SU(3), shell-model, and beyond mean-field frameworks implying that interactions between particles in the $\pi f_{5/2} p$ and νsd orbits are mostly responsible for the collectivity present.

A basic question of nuclear-structure studies is how to microscopically describe the onset of collective behavior when moving away from shell closures in terms of the interactions between individual nucleons occupying single-particle states. The rapid onset of strong quadrupole deformation in the ground states of the Sr and Zr isotopes when going from $N = 58$ to 60 neutrons has been investigated intensively [1–3]. Less is known however about the neutron-rich $A \sim 90$ nuclei north-east of ^{78}Ni which can possess collective states when just four valence protons and two neutrons are present [4]. The fragile nature of the ^{78}Ni core has been suggested as a likely reason for the presence of $(5,6^+)$ states at an energy of ~ 3 MeV in ^{82}Ge [5] and a tendency towards γ softness in ^{84}Ge [4]. Experimental data suggest the (2_1^+) state of ^{86}Ge may be deformed [6]. Recently evidence has been found for collective behavior in the neutron-rich Se isotopes, namely, the beginning of a γ band in ^{86}Se [7,8], and a $j - 1$ ground-state spin of $(3/2^+)$ for ^{87}Se [9]. The next nucleus in the Se isotopic chain ^{88}Se was reported to have an anomalously high (2_1^+)-state energy (886.2 keV) [10], compared to the systematics of the $N = 50$–54 Ge, Se, and Kr isotopes, shown in Fig. 2 of Ref. [6]. However, this 886.2-keV transition recently was reassigned to ^{87}Se [9] leaving the level scheme of ^{88}Se currently unknown.

Comprehensive shell-model (SM) and symmetry conserved configuration mixing-Gogny (SCCM) calculations have been published for ^{88}Se [11]. These predict that not only a significant amount of triaxiality should be present in ^{88}Se, but also that its ground state may have the largest axial deformation of the weakly deformed neutron-rich $A \sim 90$ region [11]. Here the collectivity arises from the quadrupole interaction between the occupied $\pi(1f_{5/2}, 2p)$ and $\nu(2d, 3s_{1/2}, 0g_{7/2})$ orbits, which can form algebraic pseudo-SU(3) symmetry blocks, driving deformation when only a few valence neutrons or protons are added to a ^{78}Ni core. Indeed the results of the SM and SCCM calculations for ^{88}Se were shown to be consistent with

an algebraic pseudo-SU(3) description in Ref. [11]. In this context, it is interesting to study the structure of ^{88}Se.

Previous prompt-γ studies of the neutron-rich Se isotopes have relied on ^{248}Cm [7,9] or ^{252}Cf [10] spontaneous-fission sources placed at the center of large arrays of Ge detectors. A more favorable fission reaction for their study is ^{235}U(n_{th}, f) where the peak of the light-mass distribution is shifted a few units of Z and A lower and the neutron-rich Se isotopes are produced with about a factor of ~ 10 greater fission yield. This reaction has been used in conjunction with the EXILL Ge array to study excited states in the neutron-rich Se nuclei and in particular construct a first level scheme of ^{88}Se.

The experiment was carried out at the PF1B cold-neutron beam [12] of the Institute Laue-Langevin in Grenoble using the EXILL array of Ge detectors [13]. Here a collimated 12-mm diameter beam of cold neutrons [14] was incident on a ^{235}U target producing fission reactions. Targets with masses of 0.525 and 0.675 mg were irradiated separately in two consecutive runs. The ^{235}U in the first target was sandwiched between thick Zr foils and in the second between thick Be foils. These backings stopped the fission fragments in a time of just a few picoseconds, and identical Doppler broadening was observed for transitions emitted by in-flight fission fragments for both targets. The thermal-equivalent neutron flux was $\sim 1 \times 10^8$ $n\,\text{s}^{-1}\,\text{cm}^{-2}$, giving a fission rate of $\sim 1 \times 10^5$ s^{-1}. The target was placed at the center of the EXILL array, which consisted of eight Compton-suppressed EXOGAM Clover detectors [15] placed on the plane perpendicular to the neutron beam. The array was completed by six Compton-suppressed GASP detectors [16] and two Clover detectors from the Lohengrin spectrometer. The distance between the target and the faces of the Ge detectors was ~ 15 cm.

The data were collected in a triggerless mode using a digital acquisition system with a 100-MHz clock [17], recording 8 Tb of data over 22 days. In the offline analysis, a total
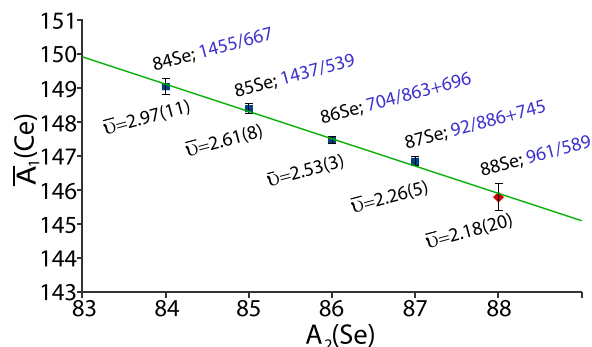
FIG. 1. Average mass of Ce partner nuclei measured with γ-ray gates set on different Se fission fragments. The gates used are labeled in blue.

of 6.6×10^{10} signals were sorted into triple- and higher-fold γ-coincidence events where a coincidence time of 200 ns was used. The higher multiplicity events were unpacked into triple coincidences [18]. Two consecutive γ-ray gates were then set in the triple coincidences to produce spectra used to search for transitions belonging to ^{88}Se.

No γ transitions are currently assigned to ^{88}Se. In order to find γ decays of this nucleus gates were set on lines belonging to its most likely complementary fission partner. For the Se isotopes these are the Ce ones as no protons are evaporated in the binary cold-neutron-induced fission of ^{235}U. To find the most abundant fission partner of ^{88}Se gates were set on known γ decays of the other Se fission fragments, and the average Ce isotope mass then was determined for each Se nucleus. The results are shown in Fig. 1, and from the gradient of this graph the nucleus of ^{146}Ce was found to be the most likely fission partner of ^{88}Se in the ^{235}U(n_{th},f) reaction.

Setting double gates on the intense $2^+ \rightarrow 0^+$ (258.2-keV) and $6^+ \rightarrow 4^+$ (502.8-keV) transitions of ^{146}Ce allowed the spectrum shown in Fig. 2 to be produced. Here one observes three lines at 704.4, 863.5, and 696.1 keV previously attributed to ^{86}Se ($4n$ channel) [7] and the 92.2-, 745.2-, 886.2-keV lines of ^{87}Se ($3n$ channel) [9] along with other transitions from ^{146}Ce [19]. There are three unidentified lines at 589.4, 961.9, and 1242.5 keV, which are investigated in more detail below.

A double gate was then set on the new 589.4- and 961.9-keV lines, and strong γ-ray transitions from the complementary fragments of $^{145-147}$Ce were present, allowing the 589.4–961.9-keV cascade to be assigned to a Se isotope. An unknown transition at 1156.6 keV is also present in Fig. 3 and is placed in cascade with the 589.4- and 961.9-keV lines. The average mass of the Ce isotopes in coincidence with the 589.4–961.9-keV double gate was measured to be 145.8(2). This data point is shown in red in Fig. 1 and establishes that the 589.4–961.9-keV cascade belongs to ^{88}Se.

When setting the same gates on ^{88}Se as those used in Fig. 3, decays from the first excited state in ^{146}Ce were measured to have more than three times the intensity of those from ^{145,147}Ce after correction for internal conversion. Gating individually on two equivalent transitions in ^{86}Se and ^{87}Se resulted in almost equally measured decay intensities from ^{147,148}Ce and ^{146,147}Ce, respectively. These three intensity distributions are
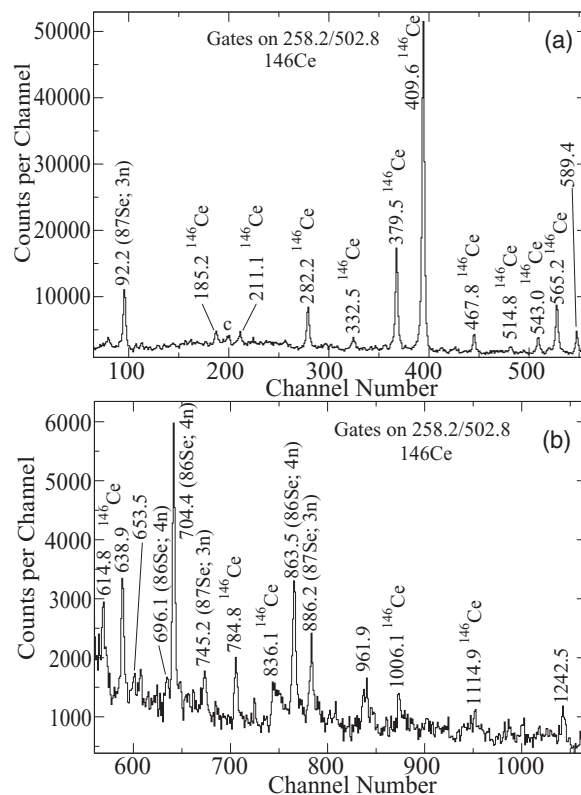

FIG. 2. Two γ-ray coincidence spectra obtained by double gating on the 258.2- and 502.8-keV γ-ray transitions in ^{146}Ce: showing a range (a) between 50 and 600 keV and (b) between 600 and 1250 keV. Contaminant lines are labeled with c.

all consistent with $\sim$2.4 neutrons being emitted on average per ^{235}U(n_{th},f) reaction [20] and the mass assignments shown in Fig. 1.

Gates were then set on the new 1242.5-keV line, and the strongest transitions of ^{146}Ce and the resulting spectra summed. A new 556.1-keV transition was observed. Gating on this decay and the 1242.5-keV line produced the spectrum shown in Fig. 4. Transitions from two Ce isotopes are present
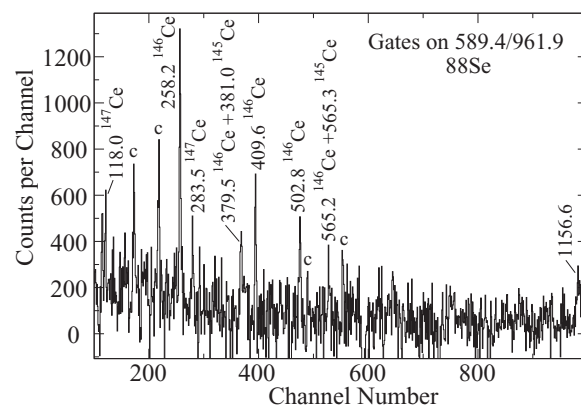

FIG. 3. Coincidence γ-ray spectrum obtained by double gating on the 589.4- and 961.9-keV lines. Contaminant lines are labeled with c.
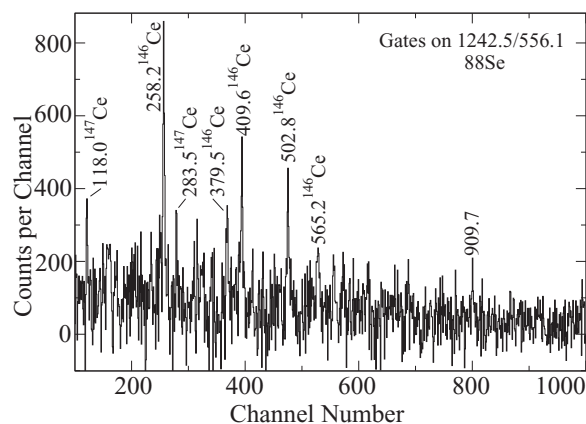
FIG. 4. Coincidence spectrum created by double gating on the new 1242.5- and 556.1-keV transitions.

along with a weak unknown line at 909.7 keV. The sum of the 1242.5-, 556.1-, and 909.7-keV transitions is 2708.3 keV, the same as the sum of the 589.4-, 961.9-, and 1156.6-keV lines. These two sets of three transitions are therefore placed parallel in the decay scheme. The new 653.5-keV transition present in Fig. 2 is the difference between the 1242.5- and the 589.4-keV γ rays, linking the two cascades.

The above coincidence relationships and further gating have allowed the decay scheme of ^{88}Se shown in Fig. 5 to be constructed. The order of the transitions in the yrast band was determined from their measured intensities when the gates were set only on the decays of ^{146}Ce. The similar energy of the (4_1^+) state in ^{86}Se [7] has allowed the same tentative spin assignment to be proposed for the 1551.3-keV level.

The 1242.5-keV state of ^{88}Se is assigned a spin of (2_2^+) due to the close energies of the (2_2^+) levels in ^{90}Kr (1362.6 keV)
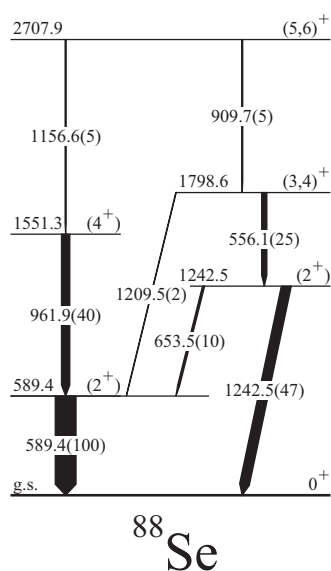

FIG. 5. Level scheme of ^{88}Se as obtained in the present Rapid Communication. The relative γ-ray intensities are given in square brackets.
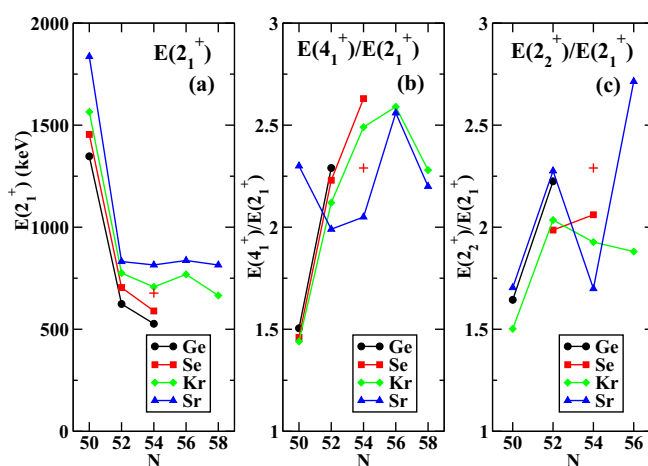

FIG. 6. (a) Experimental energies of the (2_1^+) states, (b) ratios of the level energies $E(4_1^+)/E(2_1^+)$, and (c) $E(2_2^+)/E(2_1^+)$ of $50 \leqslant N \leqslant 58$ Ge, Se, Kr, and Sr isotopes. Shell-model calculated values for ^{88}Se are highlighted by a + symbol.

[21] and ^{86}Se (1399.0 keV) [8]. It is probably the beginning of a γ band, analogous to the one reported for ^{86}Se [7,8]. However more members of this band must clearly be established before its nature can be defined.

The systematic evolution of the experimental energies of the known (2_1^+) states in the $50 \leqslant N \leqslant 58$ Ge, Se, Kr, and Sr isotopes is shown in Fig. 6(a). The 589.4-keV (2_1^+) level of ^{88}Se is situated between those of ^{86}Ge and ^{90}Kr. In Fig. 6(a) one can see that the $E(2_1^+)$ values of each isotonic chain between $N = 52$ and 58 decrease when going from Sr down to Ge, implying an increase in quadrupole deformation. The $E(4_1^+)/E(2_1^+)$ energy ratios of the Se and Kr nuclei, shown in Fig. 6(b), increase from 2.1 to 2.3 at $N = 52$, which are typical values for vibrational excitations, to 2.5 to 2.6 at $N = 54$, characteristic of γ-unstable or transitional nuclei. This increase in collectivity is confirmed by the rise in $B(E2; 2_1^+ \to 0_1^+)$ values from $\sim$10 to 20 W.u. (Weisskopf units) when going from $^{88\,\text{to}\,94}$Kr [22–24]. From their similar $E(2_1^+)$ values and $E(4_1^+)/E(2_1^+)$ ratios, it is likely that the low-energy states of ^{86,88}Se have comparable collective characteristics.

A quadrupole deformation of $\beta = 0.24(2)$ was derived for ^{86}Ge in Ref. [6] using Raman's empirical formula, which relates β to $E(2_1^+)$ and mass [25]. The same equation allows $\beta = 0.22(2)$ to be estimated for ^{88}Se. These two deformations are larger than $\beta_2 = 0.17$ calculated by the finite range droplet model [26] for both nuclei, possibly pointing to a faster onset of deformation than expected. It is also worth noting that the $E(4_1^+)/E(2_1^+)$ ratio for ^{88}Se shown in Fig. 6(b) is the highest one so far reported in this region pointing to increased rigidity. The increased quadrupole deformation and rigidity of the Ge and Se members of each $52 \geqslant N \geqslant 56$ isotonic chain, compared to their Kr and Sr counterparts, implies that the $Z = 38$ or 40 subshell closures play a role in generating a softer shape. Furthermore Figs. 6(b) and 6(c) show that the $N = 56$ subshell has the most pronounced effects for the Sr nuclei.
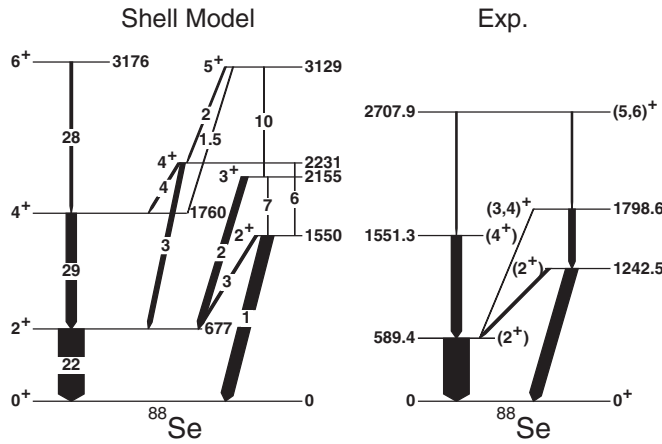
FIG. 7. Calculated and experimental energies of excited states in ^{88}Se. Linewidths represent transition intensities, including any $M1$ and $E2$ components. $B(E2)$ values in W.u. are labeled on the arrows. See the text for more details.

The (2_2^+) level energy of ^{88}Se is the lowest one known in the region. It lies below the (4_1^+) state, indicating triaxial softness. However, the data in Fig. 6(c) show that several other nuclei in the region appear to be softer towards triaxial deformation.

To further investigate the properties of ^{88}Se the experimental level scheme has been compared to the results of a SM calculation displayed in Fig. 7. The valence space used is composed of the $\pi f_{5/2}$, $\pi p_{3/2}$, $\pi p_{1/2}$, $\pi g_{9/2}$, $\nu d_{5/2}$, $\nu d_{3/2}$, $\nu s_{1/2}$, $\nu g_{7/2}$, and $\nu h_{11/2}$ orbits. A recent effective interaction for this model space (Ni78-II) has been employed. This effective interaction and its previous version (Ni78-I) have successfully described the structure of one or more $A \sim 90$ nuclei in each of the $Z = 32$–40 isotopic chains [2,7,8,27–30]. Compared to the SM calculations of ^{88}Se presented in Ref. [11], which used the Ni78-I effective interaction, the $\pi f_{5/2}$-$\pi p_{3/2}$ single-particle energy splitting has been reduced in light of recent experimental data. The Ni78-II effective interaction includes a revised fit of the π-π matrix elements, performed using a linear combination method, to reproduce the available data on the $N = 50$ isotones [27]. The results presented in Fig. 7 supersede the ones for ^{88}Se described in Ref. [11]. The main changes to the calculated level scheme of ^{88}Se are that the β- and γ-bandhead states are $\sim$500-keV lower, although the energies of other members of the γ band decrease by only 150–250 keV. The 4_1^+ and 6_1^+ states descend by $\sim$200 and 400 keV too, respectively.

The general features of the experimental level scheme of ^{88}Se are reproduced reasonably well by the calculation, including the $E(4_1^+)/E(2_1^+)$ and $E(2_2^+)/E(2_1^+)$ ratios, which are marked by crosses in Figs. 6(b) and 6(c), although some collectivity is missing. The agreement between the experimental and the calculated $E(2_1^+)$, $E(2_2^+)$, and $E(4_1^+)$ values is within the typical errors, although this worsens for higher-energy states. Figure 7 also shows the predicted transition intensities as arrow widths, and these include any contributions from both $E2$ and $M1$ multipolarities. The sum of the arrow widths out of each theoretical level is the same as that of its experimental counterpart and the

agreement is mostly good. Effective charges of $e_\pi = 1.7e$ and $e_\nu = 0.7e$ were used, the same as in previous works using both the Ni78-I and the Ni78-II interactions [11,30]. The spin part of the $M1$ operator was quenched to $g_s = 0.75g_{\text{free}}$. Applying Kumar's formula [31] to the SM $B(E2)$ values allows the intrinsic shape parameter $\beta = 0.23$ to be obtained for the ground state, consistent with the empirically derived one. The calculated level sequence with a doublet of $3^+, 4_2^+$ states is characteristic of a γ-unstable nucleus. This feature, however, is not confirmed in the present experimental scheme, likely due to fission favoring the population of yrast states.

When moving away from the $Z = 28$ and $N = 50$ shell closures the $\pi f_{5/2}$, $\pi p_{3/2}$ and $\nu d_{5/2}$, $\nu s_{1/2}$ orbits are the first to be filled. These pairs of orbits form the algebraic quasi-SU(3) symmetry. The proximity of the $\pi p_{1/2}$ and $\nu d_{3/2}, g_{7/2}$ orbits would lead to two pseudo-SU(3) blocks, considered in Ref. [11], and shown to be consistent with the SM diagonalization results for ^{88}Se. An inspection of the SM wave functions shows that the πpf and νsd orbits are dominant and seem to be mostly responsible for the collectivity present in ^{88}Se. These conclusions are in line with recent results on neighboring nuclei where SM calculations have shown that the collectivity present in the low-lying states of ^{87}Se and ^{88}Br is due to the $\nu d_{5/2}^3$ configuration [9,27] and in particular its coupling to $\pi 2^+$ states. Interestingly the semimagic $N = 50$ nuclei ^{82}Ge, ^{84}Se, and ^{86}Kr all have $B(E2; 0^+ \rightarrow 2^+) \sim$ 10 W.u. [32], demonstrating the contribution of interactions only between the valence protons to the collectivity.

The high effective charges used for the SM calculations of the $B(E2)$ values indicate that orbits from outside the valence space also contribute to the collectivity present in ^{88}Se. A quadrupole deformation of $\beta = 0.22$ was determined for ^{88}Se above. At this deformation the $\pi 7/2[303]$ and $\nu 9/2[404]$ extruder orbitals approach the Fermi surface at $Z = 34$ and $N = 54$ in the Nilsson diagrams. These orbitals have $\pi f_{7/2}$ and $\nu g_{9/2}$ spherical origins and are excluded from the valence space used in the SM calculations of the present Rapid Communiication. Both of these orbits can form additional quasi-SU(3) blocks, although the SM calculations show that the $\pi f_{5/2}p$ and νsd orbits account for most of the collectivity present in ^{88}Se. Monte Carlo SM techniques in a valence space, including the neutron $hf_{7/2}p_{3/2}$ orbits in addition to the pf-gds ones, successfully described the same rapid ground-state shape transition when going from ^{98}Zr to ^{100}Zr [3]. This has been shown impossible to achieve in the natural valence space outside the ^{78}Ni core [2]. Thus the use of such larger model spaces may provide insight into the understanding of the collectivity present in the more exotic neutron-rich nuclei of the $A \sim 90$ region. Furthermore, the strong quadrupole deformation present in the ground states of the Sr and Zr isotopes beyond $N = 59$ seems to be generated by a different mechanism from the one studied in the present Rapid Communication.

Prompt γ-γ-γ coincidence measurements performed using the EXILL Ge array, following the cold-neutron induced fission of a ^{235}U target, have allowed a first level scheme of ^{88}Se to be established. The energies of the (2_1^+) and (4_1^+) states are

characteristic of a γ-unstable or transitional nucleus and hint at an increase in collectivity compared to ^{86}Se. The identification of a low-lying (2_2^+) level indicates the presence of γ vibrations in this nucleus, whereas the $E(2_1^+)$ value allowed $\beta_2 = 0.22(2)$ to be extracted empirically. Shell-model predictions were found to reproduce many of the general properties of the ^{88}Se level scheme. Previously obtained theoretical results with the pseudo-SU(3) symmetry, SM, and SCCM calculations are all consistent with each other. The SM calculations show that the $\pi f_{5/2}p$ and νsd orbits are mostly responsible for the collectivity present in ^{88}Se.

[1] K. Heyde and J. L. Wood, Rev. Mod. Phys. **83**, 1467 (2011).

[2] K. Sieja, F. Nowacki, K. Langanke, and G. Martínez-Pinedo, Phys. Rev. C **79**, 064310 (2009).

[3] T. Togashi, Y. Tsunoda, T. Otsuka, and N. Shimizu, Phys. Rev. Lett. **117**, 172502 (2016).

[4] M. Lebois *et al.*, Phys. Rev. C **80**, 044308 (2009).

[5] T. Rząca-Urban, W. Urban, J. L. Durell, A. G. Smith, and I. Ahmad, Phys. Rev. C **76**, 027302 (2007).

[6] K. Miernik *et al.*, Phys. Rev. Lett. **111**, 132502 (2013).

[7] M. Czerwiński *et al.*, Phys. Rev. C **88**, 044314 (2013).

[8] T. Materna *et al.*, Phys. Rev. C **92**, 034305 (2015).

[9] T. Rząca-Urban *et al.*, Phys. Rev. C **88**, 034302 (2013).

[10] E. F. Jones *et al.*, Phys. Rev. C **73**, 017301 (2006).

[11] K. Sieja, T. R. Rodríguez, K. Kolos, and D. Verney, Phys. Rev. C **88**, 034327 (2013).

[12] H. Abele *et al.*, Nucl. Instrum. Methods Phys. Res., Sect. A **562**, 407 (2006).

[13] A. Blanc *et al.*, EPJ Web Conf. **93**, 01015 (2015).

[14] W. Urban *et al.*, J. Instrum. **8**, P03014 (2013).

[15] J. Simpson *et al.*, Acta Phys. Hung. N.S., Heavy Ions **11**, 159 (2000).

[16] http://gasp.lnl.infn.it/.

[17] P. Mutti *et al.*, *ANIMA 2013 3rd International Conference, Marseille, 2013* (IEEE, Piscataway, NJ, 2013), p. 1.

[18] I. Ahmad and W. R. Phillips, Rep. Prog. Phys. **58**, 1415 (1995).

[19] W. Phillips *et al.*, Phys. Lett. B **212**, 402 (1988).

[20] J. Hopkins and B. Diven, Nucl. Phys. **48**, 433 (1963).

[21] T. Rząca-Urban *et al.*, Eur. Phys. J. A **9**, 165 (2000).

[22] D. Mucher *et al.*, Prog. Part. Nucl. Phys. **59**, 361 (2007).

[23] J.-M. Régis *et al.*, Phys. Rev. C **90**, 067301 (2014).

[24] M. Albers *et al.*, Nucl. Phys. A **899**, 1 (2013).

[25] S. Raman, C. W. Nester, and P. Tikkanen, At. Data Nucl. Data Tables **78**, 1 (2001).

[26] P. Möller, A. Sierk, T. Ichikawa, and H. Sagawa, At. Data Nucl. Data Tables **109-110**, 1 (2016).

[27] M. Czerwiński *et al.*, Phys. Rev. C **92**, 014328 (2015).

[28] G. S. Simpson *et al.*, Phys. Rev. C **82**, 024302 (2010).

[29] W. Urban *et al.*, Phys. Rev. C **85**, 014329 (2012).

[30] J. Litzinger *et al.*, Phys. Rev. C **92**, 064322 (2015).

[31] K. Kumar, Phys. Rev. Lett. **28**, 249 (1972).

[32] B. Pritychenko, M. Birch, B. Singh, and M. Horoi, At. Data Nucl. Data Tables **107**, 1 (2016).